Faraday Discussions

Accepted Manuscript

This manuscript will be presented and discussed at a forthcoming Faraday Discussion meeting. All delegates can contribute to the discussion which will be included in the final volume.

Register now to attend! Full details of all upcoming meetings: http://rsc.li/fd-upcoming-meetings

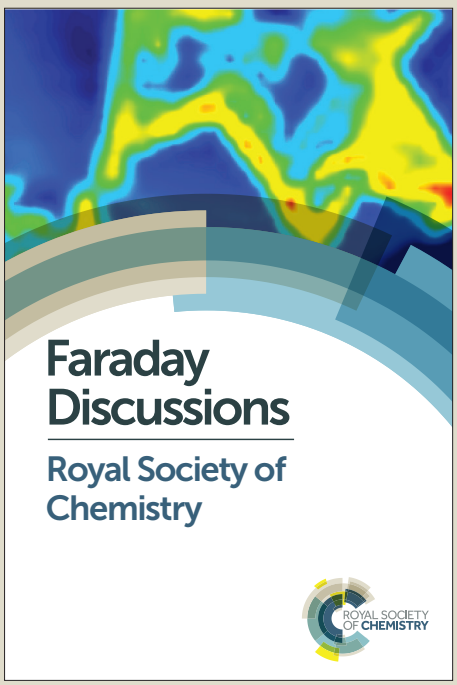

This is an *Accepted Manuscript*, which has been through the Royal Society of Chemistry peer review process and has been accepted for publication.

Accepted Manuscripts are published online shortly after acceptance, before technical editing, formatting and proof reading. Using this free service, authors can make their results available to the community, in citable form, before we publish the edited article. We will replace this *Accepted Manuscript* with the edited and formatted *Advance Article* as soon as it is available.

You can find more information about *Accepted Manuscripts* in the Information for Authors.

Please note that technical editing may introduce minor changes to the text and/or graphics, which may alter content. The journal's standard Terms & Conditions and the Ethical guidelines still apply. In no event shall the Royal Society of Chemistry be held responsible for any errors or omissions in this *Accepted Manuscript* or any consequences arising from the use of any information it contains.

ROYAL SOCIETY OF CHEMISTRY

www.rsc.org/faraday_d

Journal Name

ARTICLE

Supramolecular photochemistry applied to artificial photosynthesis and molecular logic devices

Devens Gust[a]

Received 00th January 20xx,
Accepted 00th January 20xx
DOI: 10.1039/x0xx00000x

Supramolecular photochemical systems consist of photochemically active components such as chromophores, electron donors or electron acceptors that are associated via non-covalent or covalent interactions and that interact in some functional way. Examples of interactions are singlet-singlet energy transfer, triplet-triplet energy transfer, photoinduced electron transfer, quantum coherence and spin-spin magnetic interactions. Supramolecular photochemical "devices" may have applications in areas such as solar energy conversion, molecular logic, computation and data storage, biomedicine, sensing, imaging, and displays. This short review illustrates supramolecular photochemistry with examples drawn from artificial photosynthesis, molecular logic, analog photochemical devices and models for avian magnetic orientation.

Introduction

What is supramolecular photochemistry? This short review will answer the question through selected examples. As defined by Jean-Marie Lehn in his Nobel lecture in 1987, "Supramolecular chemistry is the chemistry of the intermolecular bond, covering the structures and functions of the entities formed by association of two or more chemical species."[1] Thus, supramolecular photochemistry includes the photochemical properties of molecular entities that associate by non-covalent interactions such as hydrogen bonding, electrostatic effects, etc. However, supramolecular photochemistry is more inclusive. A chromophore is not defined by the molecule in which it resides, but rather by a substructure over which most of the excitation energy resulting from light absorption extends. Typically, this is a delocalized π-electron system or a metal complex. Similarly, electron accepting or donating species are also demarcated by conjugated π-electron systems, metal centres, etc. Thus, Balzani and co-workers have defined supramolecular photochemistry to describe "an appropriate assembly of suitable molecular components capable of performing light-induced functions," i.e., a "photochemical molecular device," whether the functional components are joined by intermolecular forces or covalent bridges.[2] Indeed, a large number of the contributions to the 1987 book *Supramolecular Photochemistry*, edited by Balzani, deal with covalently linked systems.[3] This expanded definition is logical because the interactions between the chromophores and other components of such a photochemical molecular device are determined in large part by their separations, orientations, and electronic coupling interactions, whether these are in turn controlled by covalent or non-covalent interactions.

In this contribution, I will illustrate supramolecular photochemistry by using examples from artificial photosynthesis and from molecular logic. Most of these examples come from our laboratories, and most deal with chromophores joined by covalent linkers.

Mechanisms of component interaction

Supramolecular photochemistry is not of interest simply because several chromophores and sometimes other functional components are associated with one another in some way, but rather because they communicate with one another – they interact. Before considering examples of supramolecular photochemistry, we will examine some types of interactions.

Singlet-singlet energy transfer

[a] *Department of Chemistry and Biochemistry, Arizona State University, Tempe, AZ, 85287. E-mail: gust@asu.edu.*
See DOI: 10.1039/x0xx00000x

A chromophore in its first excited singlet state, generated upon light absorption, will always decay by the intrachromophoric processes of internal conversion and vibrational relaxation to the ground state, fluorescence, and intersystem crossing to the triplet manifold. However, if there is another chromophore of the same or different type close enough for interchromophore interaction, decay may also occur by singlet-singlet energy transfer. In this nonradiative, resonant process, the energy donor chromophore returns to the ground state with concurrent transfer of excitation energy to the acceptor, generating an excited singlet state of the acceptor. Usually, this process occurs by the Förster dipole-dipole mechanism or some variation thereof. [4,5] The rate, and therefore the efficiency, of energy transfer depends mainly upon the oscillator strengths of the relevant transitions in the donor and the acceptor, the spectral overlap of the transitions (because energy transfer is a resonant process), and the separation and relative orientation of the transition dipoles. The separation and orientation are determined by the forces that control the structure of the system, whether they are covalent or non-covalent. The rate constant for singlet-singlet energy transfer depends on the negative 6th power of the separation of the transition dipoles.

Electron transfer

A chromophore and associated donor or acceptor moiety may interact by photoinduced electron transfer. An excited state is both a better electron donor than the ground state and a better electron acceptor, and so an excited chromophore can either donate an electron to an acceptor or accept an electron from a nearby donor to form a charge-separated state. Such a state may recombine to the ground state, or undergo a charge shift reaction in which the radical ion pair donates an electron to a secondary acceptor or accepts an electron from a secondary donor.

A theoretical framework for electron transfer, as represented by eq. 1, was developed by Marcus, Hush, and Levitch,[6-11] and since elaborated by many others. The electron transfer rate constant k_{et} is a function of the temperature and three other variables.

$$k_{et} = \sqrt{(\frac{\pi}{\hbar^2 \lambda k_B T})}[V]^2 exp[-(\Delta G^0 + \lambda)^2/4\lambda k_B T] \quad (1)$$

The free energy change for the reaction, ΔG^0, can be estimated from the redox potentials of the donor and acceptor in their ground states and, in the case of photoinduced electron transfer, the energy of the excited state relative to the ground state. The reorganization energy λ is the sum of the internal reorganization energy λ_i (which is associated with molecular structural differences between the initial and final states) and the solvent reorganization energy λ_s (which is associated with differences in solvation of the initial and final states).

The electronic coupling between the initial and final states, $|V|^2$ is related to the overlap of electronic orbitals on the donor and the acceptor, and is therefore a function of the separation of the donor and acceptor. In the case of covalently linked systems, the coupling is often controlled by the linkage bonds (superexchange).[12] In this mechanism, the linker orbitals overlap with those of the donor and acceptor and thereby increase coupling. Often, the rate is an exponential function of the separation, or nearly so.

Triplet-triplet energy transfer

The excited triplet state of a chromophore may transfer triplet excitation energy to an acceptor chromophore whose lowest-lying triplet state is at the same or lower energy. The Förster mechanism is ineffective for triplet transfer because transitions between a triplet and a singlet ground state violate the Wigner spin conservation rules, and have very low oscillator strengths. Triplet-triplet transfer usually occurs by the Dexter mechanism,[13] which involves overlap of the relevant orbitals in the donor and the acceptor. The process can be envisioned as a double electron exchange in which an electron in the LUMO of the donor migrates to the LUMO of the acceptor while an electron in the HOMO of the acceptor concurrently migrates to the HOMO of the donor. In this way, Dexter transfer is related to photoinduced electron transfer.

The rate constant for triplet-triplet transfer depends on a spectral overlap term (energy term) and the electronic coupling between the initial and final states. In donors and acceptors that are not covalently linked, or are linked by long, insulating linkages, the distance dependence of triplet-triplet transfer is exponential, as the "tails" of electronic orbitals tend to decay exponentially with distance. Rapid transfer requires the donor and acceptor to be at near-collisional separations (less than about 10 Å. In systems with less-insulating covalent linkages, transfer can occur by involvement of the linkage bonds, as in electron transfer.

Quantum coherence and related effects

If the association between two chromophores in a supramolecular complex is strong enough, electronic excitation can move from chromophore to chromophore as quantum mechanical wave packets that maintain their phase coherence.[14,15] Such quantum coherence effects have been invoked in photosynthetic pigment complexes, where they may allow singlet energy transfer to be rapid enough to compete with the loss of excitation energy by other mechanisms.[16,17]

Photoinduced charge separation often generates a biradical. If the electrons on the donor and the acceptor of the radical pair are close enough together to couple magnetically, their spins will interact, generating singlet and/or triplet biradicals. This is of interest because while singlet biradicals can recombine to give the ground electronic state, triplet biradicals can only recombine to give excited triplet states. The rate of recombination of the biradical charge separated state and the ratio of recombination to

the singlet and triplet states is controlled by magnetic interactions between the two electron spins and with other magnetic fields, and not by the usual thermal energies. External magnetic field effects on charge recombination[18,19] have been observed in the supramolecular structures of photosynthetic reaction centres,[20-23] and in artificial systems. It is likely that one of the mechanisms by which some birds and other organisms navigate and orient using the earth's magnetic field is this so-called "radical pair effect." As we shall see, similar effects at low magnetic fields have been observed in artificial supramolecular photochemical systems.[24-26]

Environmental effects on single chromophores

A chromophore may interact with another component of a supramolecular system in such a way that its change in environment affects the photochemistry. Examples are environmental changes that affect the spectroscopic properties of the chromophore and spatial localization of the chromophore. These kinds of changes can be useful in sensing and imaging applications.

Supramolecular photochemistry in artificial photosynthesis

The photosynthetic apparatus of green plants and other organisms is a complex supramolecular photochemical device that absorbs sunlight, converts the resulting excitation energy to chemical potential energy stored in a charge-separated state, and uses this redox potential to power catalysts for fuel production, such as water oxidation catalysts and carbon dioxide reduction enzymes. Photosynthesis is thus far the only practical method of converting sunlight to energy stored in reduced carbon fuels, and is responsible for powering life on earth and for production of the fossil fuels that account for most of the technological energy used by humans. The initial steps of photosynthesis are relatively efficient, although some of the later catalytic steps are not.

Given the success and importance of photosynthesis, it is not surprising that the process has inspired a great deal of research into artificial photosynthesis. Artificial photosynthesis is the application of the fundamental science underlying photosynthesis to the design of technological systems for converting sunlight into energy stored in a fuel. The idea dates back at least to the beginning of the 19th century, when Giacomo Ciamician championed the idea of replacing energy from coal with energy from artificial photosynthesis.[27] Although neither the science of photochemistry nor biological knowledge were sufficient to allow dramatic progress in artificial photosynthesis in the time of Ciamician, the last 40 years have seen very significant advances, and solar fuels such as hydrogen can be produced in the laboratory. However, practical artificial photosynthesis has still not been achieved.

Photosynthesis is a modular process wherein different proteins carry out the functions of light gathering, charge separation, catalysis, regulation and photoprotection. These proteins are organized into a supramolecular structure by the photosynthetic membrane, a lipid bilayer membrane. Thus, a promising approach to artificial photosynthesis is to create modular components, each of which can carry out one or more energy conversion functions, and to organize them into larger systems. In many approaches, the components are molecular, in many others they are materials-based, and in yet others they are a combination of the two. Below, we present a few examples of supramolecular photochemistry in artificial photosynthesis.

Antenna systems

Although the conversion of excitation energy to redox potential in photosynthesis occurs in the photosynthetic reaction centre, most of the light used in photosynthesis is absorbed by antenna systems. The antennas perform several services. First, they absorb light over a significant fraction of the solar spectrum, whereas a single chromophore generally absorbs only in certain spectral regions. Thus, the antennas make photosynthesis more efficient. Secondly, each reaction centre is fed excitation energy by a large number of antenna chromophores. This allows the organism to drive the multi-electron redox processes necessary for fuel production sufficiently rapidly to be efficient, even at low light levels. In addition, the antennas contain some of the photoprotective and photoregulatory processes that protect the organism from damage by light and oxidative reactions.

Because the antennas contain many chromophores (hundreds in some cases), singlet-singlet energy transfer among them and to reaction centre chromophores is the basic physical process in the antennas. Thus, artificial antennas also deal with singlet-singlet energy transfer, and their design must take into account both efficient light collection throughout the solar spectrum and the efficiency of the energy transfer processes. Efficiency in turn depends on the various factors discussed above.

Fig. 1 shows molecular hexad **1**, which is an artificial photosynthetic antenna system.[28] Six chromophores are organized into one supramolecular structure by a hexaphenylbenzene scaffold. The six phenyl rings surrounding the central benzene are relatively rigidly oriented at close to 90° angles to the central ring, and the chromophores are linked to this ring with bonds that rigidly fix the bond angles and lengths. Rotational motions that change dihedral angles are possible. Thus, the hexaphenylbenzene core controls the distances and some of the angles that are important for establishing the rates of singlet-singlet energy transfer among the chromophores.

The chromophores themselves have been chosen to absorb and emit in complementary spectral regions in order to achieve absorption of sunlight over a broad spectral region while ensuring good spectral overlap of donor emission and acceptor absorbance for singlet energy transfer. Fig. 2 shows part of the absorption spectra of the three different chromophores of

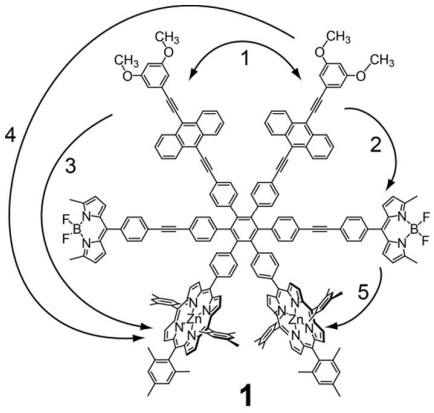

Fig. 1. Artificial photosynthetic antenna consisting of two bis(phenylethylyl)anthracene blue light absorbing chromophores, two borondipyrromethene green light absorbing chromophores, and two red light absorbing zinc porphyrin chromophores. The arrows indicate singlet energy transfer pathways.

antenna **1**. The bis(phenylethynyl)anthracene (BPEA) antennas absorb strongly in the blue spectral region from 400 – 500 nm. The two borondipyrromethene (BDPY) chromophores show absorption in the 450 – 550 and 330 - 430 nm ranges. Finally, the two zinc porphyrin moieties absorb strongly in the Soret region around 425 nm and in the Q-band region from 530 – 625 nm. The spectrum of the hexad is essentially a linear combination of the spectra of the component chromophores. Thus, the hexad can harvest sunlight throughout the visible spectral region.

The hexad was designed to function as an excitation energy funnel, wherein the BPEA would transfer singlet excitation energy to the BDPY, which in turn would pass excitation to the porphyrins. Thus, all excitation would end up in the porphyrin moieties. To achieve this, the emission spectrum of each donor chromophore must overlap the absorption of its designated acceptor. The BPEA has emission maxima at 483, 515 and ~547 (sh) nm. Thus it is energetically poised to transfer excitation to the BDPY (Fig. 2). The BDPY in turn fluoresces at 534 and ~563 nm (sh), and this emission overlaps well with the porphyrin Q-band absorption. Thus, from an energetic point of view, hexad **1** is well set up for singlet energy transfer. In addition, the BPEA and BDPY are strong fluorophores, which makes them good energy donors. The distances separating the chromophores and their relative orientations are favourable for rapid energy transfer by the Förster mechanism.

Transient spectroscopic experiments with **1** and model systems allowed determination of the rates of singlet energy transfer among the component chromophores.[28] Excitation energy was exchanged between the two BPEA units with a time constant τ of 0.4 ps. Transfer from BPEA to BDPY (step 2 in Fig. 1) occurred with τ = 5 - 14 ps. Multiple lifetimes are ascribed to multiple conformations of the BDPY. The BDPY passes excitation on to the porphyrins (step 5) with τ = 4 – 20 ps, again due to its multiple conformations. Thus, the hexad acts as an excitation energy funnel, rapidly moving excitation down an energy gradient from BPEA to BDPY to the porphyrins. In addition, it was found that BPEA can transfer excitation directly to the two porphyrins (steps 3 and 4) with time constants of 7 and 6 ps, respectively. All of these energy transfer processes are much faster than decay of the chromophore excited states by other pathways (which occurs on the ns time scale), and so the efficiency of energy transfer to the porphyrins is close to unity, no matter where the light is absorbed.

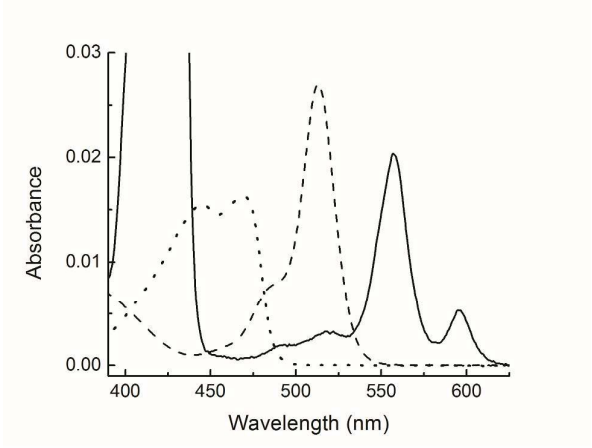

Fig. 2. Absorption spectra of models for the component chromophores of hexad antenna **1** in 2-methyltetrahydrofuran: model porphyrin (solid), model BPEA (dotted), model BDPY (dashed).

Artificial photosynthetic antenna hexad **1** performs well, collecting light over most of the visible solar spectrum and transferring it to the porphyrin moieties with high efficiency. However, it contains many fewer chromophores than typical natural photosynthetic antenna systems.

Reaction centres

Photosynthetic reaction centres use the excitation energy transferred to them by antennas to carry out photoinduced electron transfer and thereby store some of the excitation as redox potential. In all reaction centres, the photoexcited primary electron donors are chlorophylls or bacteriochlorophylls. The ultimate electron acceptor is a quinone moiety, and the result of charge separation in the reaction centre is a (bacterio)chlorophyll radical cation and a quinone radical anion. Thus, it would seem logical that the simplest type of artificial photosynthetic reaction centre would consist of an electron donor chromophore covalently linked or otherwise associated with an electron acceptor moiety in such a way that photoinduced electron transfer would be rapid. The first molecules of this type were reported in the late 1970's by Loach and coworkers,[29-31] and by Tabushi and coworkers.[32] More recent molecular artificial reaction centre **2** illustrates the principle (Fig. 3).

Molecule **2** consists of two equivalent zinc porphyrin light absorbers and electron donors linked to a single fullerene electron acceptor in a large, 42-atom macrocyclic arrangement.[33] In designing this molecule, the donors and acceptor were chosen to provide sufficient thermodynamic driving force to promote photoinduced electron transfer from the porphyrin (P) first excited singlet state to the fullerene (C_{60}) while preserving most of the excitation energy as chemical potential in the charge-separated state.

Cyclic voltammetric experiments yielded a first oxidation potential of the zinc porphyrin at 0.78 V vs SCE and a first reduction potential of the fullerene at -0.68 V. Thus, the charge-separated state energy is about 1.46 eV above the ground state. The energy of the zinc porphyrin first excited singlet state is 2.06 eV, and therefore the driving force for photoinduced electron transfer to form $P^{\bullet+}$-$C_{60}^{\bullet-}$-P from the excited state of either porphyrin is about 500 meV. The fullerene first excited singlet state lies at 1.71 eV, giving a driving force for electron transfer to this excited state of 250 meV.

Transient spectroscopy in 2-methyltetrahydrofuran allowed determination of the rate constants and quantum yields for photoinduced electron transfer. The rate constant for transfer from ^{1}P-C_{60}-P is 9.1×10^{11} s^{-1} (τ = 1.1 ps). The fullerene excited state, P-$^1C_{60}$-P, accepts an electron from either porphyrin with a time constant of 15 ps. The quantum yield of the charge-separated state by either pathway is 1.0. Charge recombination of $P^{\bullet+}$-$C_{60}^{\bullet-}$-P is much slower, with τ = 2.7 ns.

Molecule **2** exhibits some very interesting photochemistry. The photoinduced electron transfer steps are extremely rapid, and give the charge-separated state in high yield. On the other hand, charge recombination is about 2000 times slower than charge separation from ^{1}P-C_{60}-P. This large difference in rate constants is very desirable because in any artificial reaction centre charge separation must be rapid in order to compete with intrachromophore relaxation processes, but charge recombination should be slow so that there is time to harvest the redox energy for desired purposes. Relatively strong electronic coupling is necessary for rapid charge recombination, but a consequence of achieving this coupling is that coupling is also strong for charge recombination. In **2**, several factors favour the large difference in rate constants for the two processes. First, charge separation has a moderate driving force, and lies in the normal region of the Marcus rate constant vs. free energy change relationship (see above). The charge recombination to the ground state, on the other hand, has a large driving force and lies in the Marcus inverted region, where increased driving force leads to a *smaller* rate constant. This effect is enhanced by the fact that both porphyrins and fullerenes have small internal and solvent reorganization energies for electron transfer, and a small sensitivity of the ions to stabilization by solvent, relative to other acceptors such as quinones.[34-37] The small reorganization energy locates the photoinduced electron transfer reaction closer to the maximum of the Marcus curve, where the rate is maximized. The small λ also has the effect of moving charge recombination farther into the inverted region than it would be with an acceptor lacking this feature, and thus slows the rate.

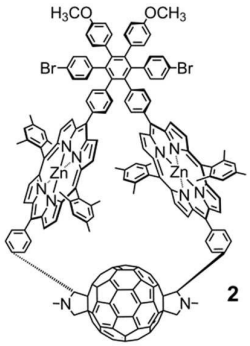

Fig. 3. Porphyrin-fullerene artificial photosynthetic reaction centre **2**.

Another factor contributing to the large rate constant difference is the very rigid structure of **2**. Molecular modelling shows that strain in the macrocycle forces the porphyrin moieties to be slightly bent, and severely limits any large scale motions of the fullerene relative to the porphyrins. This means that in the charge-separated state, the porphyrin radical cation and fullerene radical anion cannot undergo relative motions that bring them closer together, thereby increasing the electronic coupling for charge recombination.

Although charge recombination in **2** is slow relative to charge separation, the lifetime of 2.7 ns is still rather short if one wishes to couple the redox potential of the charge-separated state to catalysts for fuel production or other energy-harvesting steps. Natural photosynthesis is, of course, subject to the same physical laws as artificial systems, and faces the same problem. In natural reaction centres charge separation is stabilized in time by moving the electron through the protein across a distance that approximates the thickness of the biological membrane. In bacterial reaction centres, for example, the electron is moved from the bacteriochlorophyll special pair to quinone Q_B, which is on the other side of the membrane. At such a separation, charge recombination is very slow. From the discussion above it is apparent that photoinduced electron transfer from the (bacterio)chlorophyll excited singlet state to Q_B would be too slow to compete with decay of the (bacterio)chlorophyll excited state. In order to avoid this problem, natural reaction centres use a multistep electron transfer process to achieve charge separation that spans the membrane. In purple bacteria reaction centres, for example, the excited bacteriochlorophyll "special pair" on one side of the membrane transfers an electron to a nearby bacteriochlorophyll, which in turn donates an electron to a bacteriopheophytin. The bacteriopheophytin moves an electron on to a quinone Q_A, which transfers an electron to the final quinone Q_B on the other side of the membrane. Each step in this electron relay is fast due in part to the close proximity of the donor and acceptor, but the result of the electron transfer chain is long-range, long-lived charge separation.

It is possible to design artificial reaction centres that use this same strategy to achieve long-lived charge separation. The first such systems were reported in 1983.[38-40] The most successful of these was carotene (C) porphyrin (P) quinone (Q) molecular triad **3**[38,39] (Fig. 4). Excitation of the porphyrin in benzonitrile resulted in formation of a $C^{\bullet+}$-P-$Q^{\bullet-}$ charge-separated state with a lifetime of 420 ns and a quantum yield of 0.13. The photochemical processes that lead to this result will be illustrated with triads **4** and **5** (Fig. 4), which are similar, but feature a fullerene electron acceptor in lieu of the quinone.

The transient states of triad **4** are shown in Fig. 5. In 2-methyltetrahydrofuran solution, excitation of the porphyrin moiety of **4** yields the first excited singlet state C-^{1}P-C_{60}, which decays by photoinduced electron transfer to the fullerene (step 2 in Fig. 5) with a time constant τ of 10 ps.[41] The driving force for this step is 0.58 eV. The fullerene singlet state also decays by photoinduced electron transfer (τ = 32 ps), with a driving force of 0.31 eV. The product of photoinduced electron transfer from both C-^{1}P-C_{60} and C-P-$^1C_{60}$ is C-$P^{\bullet+}$-$C_{60}^{\bullet-}$, which is formed with a quantum yield of 0.99. At this stage, the molecule has converted light to electrochemical potential. However, based on studies of model dyads, charge recombination of C-$P^{\bullet+}$-$C_{60}^{\bullet-}$ to yield the ground state (step 3) occurs with τ = 3.3 ns. This lifetime is so short that accessing the stored redox potential via chemical reactions would be challenging. In **4**, however, a rapid shift of the positive charge to the carotene (step 4) competes with charge recombination, yielding $C^{\bullet+}$-P-$C_{60}^{\bullet-}$. The final charge-separated state has a lifetime of 170 ns and is formed with a quantum yield of 0.22.

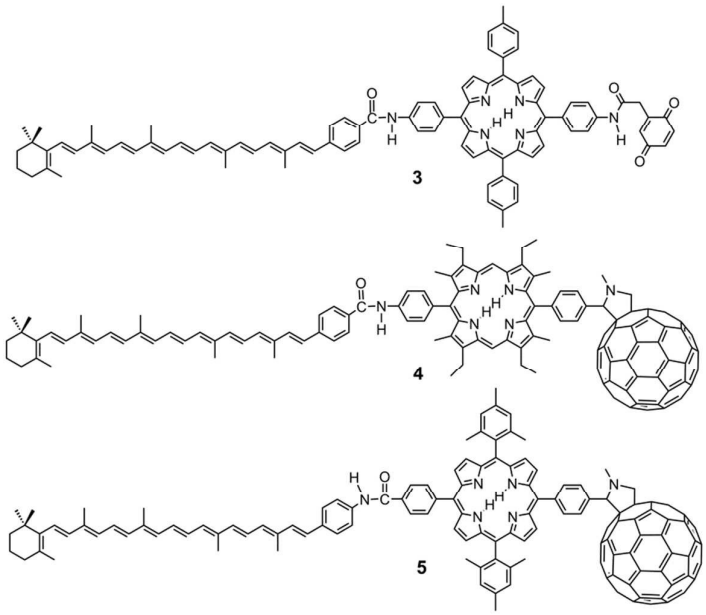

Fig. 4. Three triad artificial reaction centres.

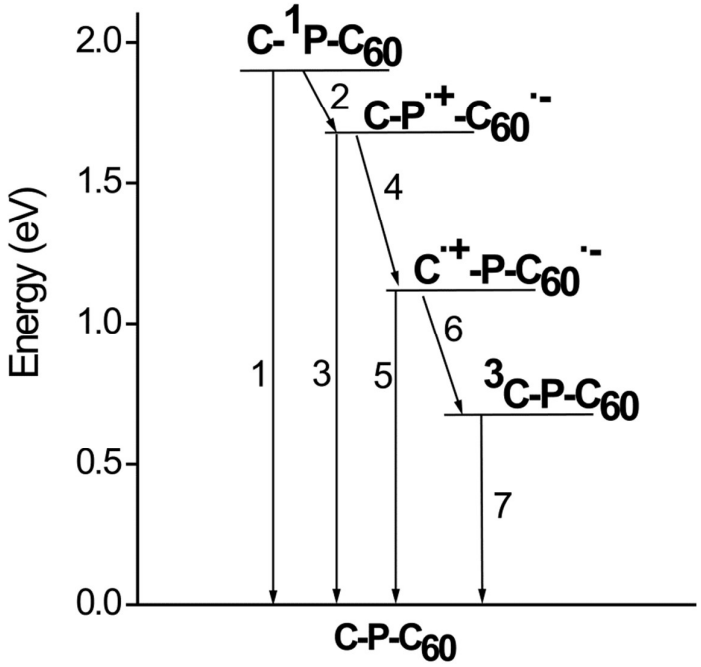

Fig. 5. Transient states and interconversion pathways for triad **4**.

The quantum yield of the $C^{\bullet+}$-P-$C_{60}^{\bullet-}$ state of **4** although improved over that of the quinone-containing triad mentioned above, is still not optimal. Using the principles of Marcus theory, we were able to tune the properties of the triad to increase the yield. Triad **5** is the result.[42] It is clear from the last paragraph that the low quantum yield of **4** is due to the fact that the ratio of rate of the charge shift step 4 in Fig. 5 to the rate of charge recombination step 3 is unfavourable. In order to make this rate more competitive, the oxidation potential of the porphyrin radical cation in **5** was increased by ca. 0.15 V by replacing the porphyrin pyrrole β-alkyl groups of **4** with *meso*-mesityl groups. In addition, the oxidation potential of the carotenoid in **5** was decreased by 0.18 V via reversal of the amide linkage to the porphyrin. These changes were expected to slow the rate of charge recombination of C-$P^{\bullet+}$-$C_{60}^{\bullet-}$ to the ground state in **5** because the reaction occurs in the inverted region of the Marcus relationship. In addition, they increased the driving force for the charge shift reaction, which was expected to increase the rate, as that reaction occurs in the normal Marcus region. The result of these structural changes is that whereas the ratio of k_4/k_3 for **4** is 0.28, the ratio for **5** is 27. For both **4** and **5**, the quantum yield of the initial C-$P^{\bullet+}$-$C_{60}^{\bullet-}$ state is essentially unity. The overall result is that although the quantum yield of the final $C^{\bullet+}$-P-$C_{60}^{\bullet-}$ state for **4** is only 0.22, that for **5** is 0.95. The electronic coupling of the moieties in the triads will also differ somewhat due to the structural changes between them, and these may also contribute to the differences in quantum yield.

During the last 30 years, a wide variety of multicomponent supramolecular constructs for photoinduced electron transfer have been reported. These employ not only porphyrins and related chromophores as the primary electron donors, but also metal complexes, which can perform in a similar fashion. Some of these systems employ more than three donor-acceptor moieties, which can extend the lifetime of the charge-separated state by further reducing coupling between the radical ions. Pentad **6**, for example, produces a charge-separated state that is reported to have a lifetime of 0.53 s at 163 K in dimethylformamide.[43] Metal complex based systems **7**[44] and **8**[45,46] have been shown to allow collection of more than one redox equivalent, which would be valuable for carrying out multi-electron redox processes for solar fuel production.

Antenna-reaction centre complexes

Artificial photosynthetic antennas and reaction centres can be associated in a functional manner to create larger supramolecular machines in which the antennas gather excitation energy and transfer it to reaction centres, where it is used to carry out photoinduced electron transfer. Key design parameters are achieving a rapid energy transfer rate from the antenna to the reaction centre, preventing energy transfer from the reaction centre back into the antenna, and preventing undesired electron or hole migration from the reaction centre into the antenna chromophores.

Many examples of antenna-reaction centre combinations have been reported. We will illustrate the idea with a representative system, **9**, (Fig. 7) which was prepared by adding dipyridylfullerene **10** to a solution of antenna **1** (Fig. 1) in 1,2-difluorobenzene.[28] The fullerene derivative self-assembles with the antenna via dative bonds to the zinc atoms in the two

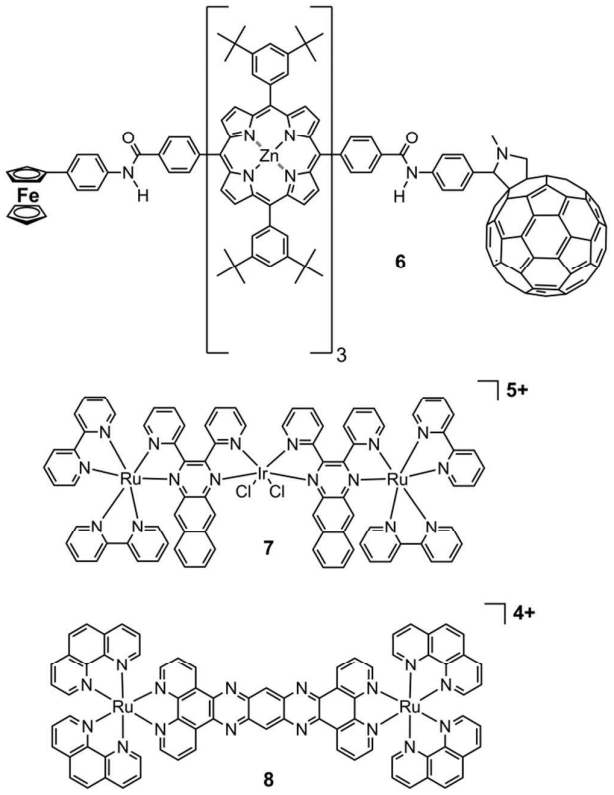

Fig. 6. Three complex artificial photosynthetic reaction centres.

porphyrin moieties. Singlet-singlet energy transfer in heptad **9** occurs with rate constants and yields essentially identical to those observed with **1** alone. Either porphyrin excited singlet state donates an electron to the fullerene with a time constant of ~3 ps to yield a $P^{\bullet+}$-$C_{60}^{\bullet-}$ charge-separated state. The state is formed with quantum yield of essentially unity, and has a lifetime of 230 ps.

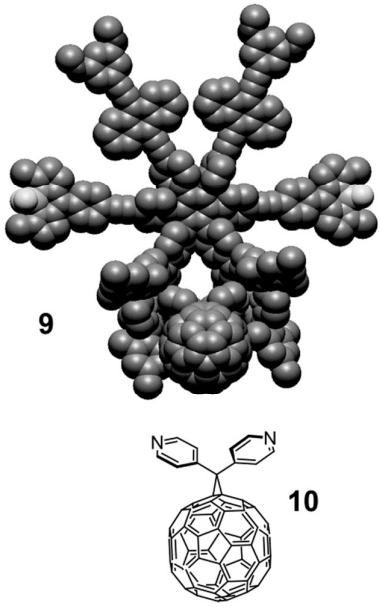

Fig. 7. Artificial antenna - photosynthetic reaction centre **9** constructed by self-assembly of fullerene **10** with antenna **1** (Fig. 1).

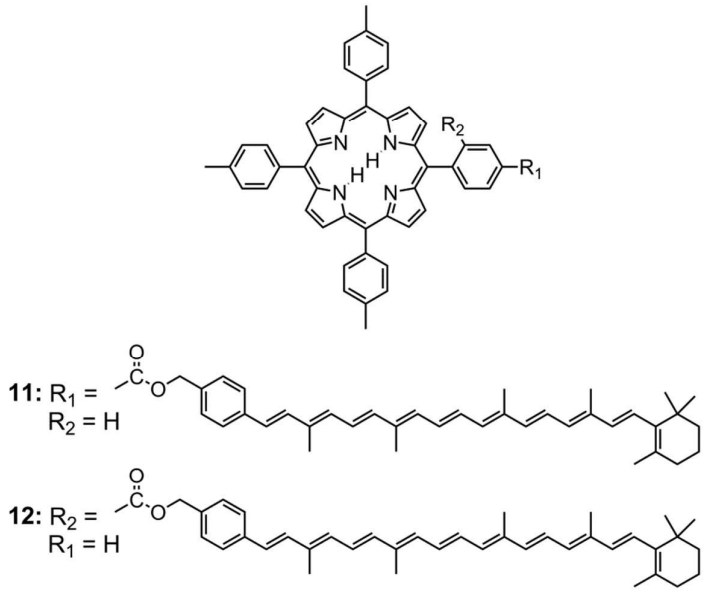

Fig. 8. Carotenoporphyrins that mimic photosynthetic carotenoid photoprotection from singlet oxygen damage.

Photoprotection

Thus far we have seen how supramolecular photochemical structures can functionally mimic some of the important features of natural photosynthesis in which the components communicate by singlet-singlet energy transfer (artificial antennas) and photoinduced electron transfer (artificial reaction centres). It turns out that a third fundamental process, triplet-triplet energy transfer, is important in mimicry of photosynthetic photoprotection.

Excited state singlet oxygen reacts rapidly with many organic compounds, including the lipids of photosynthetic membranes. Singlet oxygen is produced by reaction of the usual ground-state triplet oxygen with the triplet excited states of chlorophylls, porphyrins and other chromophores. In the reaction centres of purple bacteria, for example, the normal electron transport chain can be blocked by reduction of the quinones, whereupon the charge-separated states formed by photoinduced electron transfer cannot evolve, and instead recombine to yield bacteriochlorophyll triplet states. These states are potent sensitizers of singlet oxygen. The bacteria are protected from photodamage by singlet oxygen through the presence of carotenoid polyenes in the reaction centre. The carotenoids rapidly quench bacteriochlorophyll triplet states by a triplet-triplet energy transfer process to yield the carotenoid triplet state.[47-49] Carotenoid triplets are of too low energy to sensitize singlet oxygen production, have a short lifetime and decay harmlessly to the ground state with the evolution of heat.

Carotenoid photosynthetic photoprotection was first mimicked in a model compound in 1981[50] using carotenoporphyrins **11** and **12** (Fig. 8). Fig. 9 shows the rate of destruction of the dye diphenylisobenzofuran (DPBF) in aerated toluene solution when the solution is illuminated in the presence of various sensitizers and carotenoids.[50] The DPBF is highly sensitive to degradation by singlet oxygen. If the solution contains only a tetra-arylporphyrin sensitizer in addition to the DPBF, singlet oxygen is produced under illumination and rapidly reacts with DPBF, resulting in the bleaching of the dye (hollow circles in Fig. 9). If either of two carotenoids are added to the solution of dye and sensitizer (hollow squares and triangles), the rate of destruction of the dye decreases only slightly because at the concentrations employed (~2×10^{-6} M), diffusion-controlled triplet energy transfer from the sensitizer triplet state to carotene cannot compete with quenching of the sensitizer triplet by oxygen to generate singlet oxygen. When the carotene is covalently linked to the porphyrin as in molecule **11**, a significant decrease in the rate of photodestruction of the dye is observed because triplet-triplet energy transfer from the porphyrin triplet state to the carotenoid occurs sufficiently rapidly to reduce the triplet lifetime of the porphyrin to the point that reaction with O_2 is no longer efficient. In molecule **12**, wherein the carotenoid is folded back over the porphyrin so that the π-electron systems of the two chromophores are essentially in van der Waals contact, photoprotection is essentially complete due to very rapid quenching of the porphyrin triplet state. Time resolved measurements show that this energy transfer occurs on the time scale of a few ns or less.

Spin effects in supramolecular photochemistry

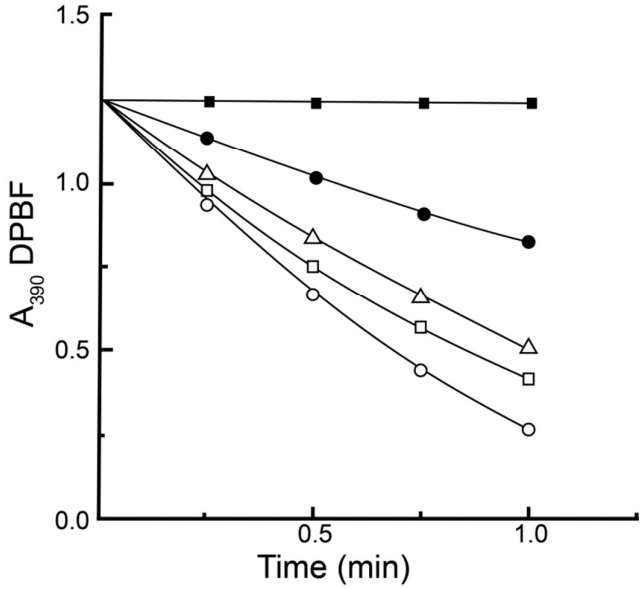

Fig. 9. Bleaching of the absorbance of the dye DPBF by reaction with singlet oxygen as a function of illumination time. The dye was dissolved in aerated toluene containing equimolar amounts of either a porphyrin sensitizer (hollow circles), the porphyrin sensitizer plus 7′-apo-7′-(4-hydroxymethylphenyl)-β-carotene (hollow squares), the porphyrin sensitizer plus β-carotene (hollow triangles), carotenoporphyrin **11** (filled circles) or carotenoporphyrin **12** (filled squares).

At least 50 species of organisms, especially birds, use the earth's magnetic field for navigation and orientation,[51] but the mechanism(s) of this biological compass are not fully understood. One possibility consistent with what is known is that birds and perhaps other organisms may use photoinduced electron transfer in supramolecular structures to generate radical pair states whose lifetimes depend on the orientation and/or magnitude of the earth's magnetic field.[52] As discussed earlier, relatively strong magnetic fields have long been known to have such effects in photosynthesis and in model systems, but there has been no evidence that fields as weak as that of the earth (~50 μT) could produce measureable effects. Recently, carotenoporphyrin fullerene triad **5** (Fig. 4) has been shown to function in this way.[25,26]

As can be seen in Fig. 5, the $C^{\bullet+}$-P-$C_{60}^{\bullet-}$ charge-separated state that is formed by photoinduced electron transfer followed by charge shift can decay either directly to the ground state via step 5, or to form the carotenoid triplet state by step 6. The $C^{\bullet+}$-P-$C_{60}^{\bullet-}$ biradical is formed in its singlet state, with the two electron spins paired. However, the spins are only weakly coupled, and the charge-separated state lives long enough that the singlet and three triplet states can interconvert via magnetic interactions such as hyperfine interactions with carotenoid protons. The singlet biradical, $^{S}[C^{\bullet+}$-P-$C_{60}^{\bullet-}]$ can recombine directly to the molecular ground state. The triplet biradical $^{T}[C^{\bullet+}$-P-$C_{60}^{\bullet-}]$, however, can recombine only to give the spectroscopic triplet state ^{3}C-P-C_{60}. The four biradical states are nearly isoenergetic, but external magnetic fields can influence the energies of the states and their interconversion rates. This in turn will affect the decay profile of the charge-separated states and the relative yields of singlet ground state and triplet state.

This effect was first reported for triad **4** with moderate magnetic fields (20 mT) at low temperature, and is reminiscent of the similar effects seen in natural photosynthetic reaction centres.[24] Building on this result, triad **5** was studied at low temperatures and magnetic fields as low as ~ 3 mT were found to give dramatic changes in the lifetime of $C^{\bullet+}$-P-$C_{60}^{\bullet-}$.[25] The orientation of the magnetic field was also varied with respect to the molecular orientation, and the magnitude of the magnetic field effect was found to be a function of the orientation of the external field, even at field strengths of ca. 3 mT. These experiments suggest that the radical pair mechanism could be the source of the avian compass, but the molecular mechanism of the effect in birds has yet to be established.

Supramolecular chemistry, molecular logic and molecular photonics

The same principles of communication among the components of supramolecular devices by energy and electron transfer that are useful in artificial photosynthesis can be employed in molecule-based digital logic and photonics. A few examples will be discussed.

Molecular logic

Photochemical switches. The transistor (and its predecessor the vacuum tube) has allowed the development of electronics and electronic data processing. A field effect transistor acts as an amplifier, in which electrical current flowing from an input (source) to an output (drain) is controlled by the voltage at a second input (gate). The transistor can be used either as an

amplifier, or as a digital on/off switch. Suitably designed supramolecular systems can behave as photochemical analogues of transistors in which the inputs and outputs are photonic, rather than electronic. Such supramolecular machines can function as binary switches and much more complex Boolean logic gates. In analogue applications, they can both act as photonic "amplifiers" and mimic the kinds of control functions found in biology.

Photochromic molecules, such as fulgimide **13** (Fig. 10), are particularly convenient examples of simple photochemical molecular switches.[53,54] Photochromes exist in two metastable isomeric forms, and light can be used to interconvert them by photoisomerization. Compound **13** is stable in solution as an open form FGo (actually a mixture of *E*- and *Z*-isomers) with an absorption maximum at 380 nm. Irradiation with blue light, for example 366 nm, leads to photocyclization to the closed isomer FGc. A photostationary distribution consisting of mainly FGc results, and displays absorption maxima at 400 and 510 nm. Photochrome FGc fluoresces (λ_{max} = 600 nm). Irradiation of FGc in the visible (e.g. 560 nm) results in photoisomerization back to FGo. Thus, **13** is a photochemically operated molecular switch whose inputs and outputs are light.

Photochemical logic gates. Boolean logic gates employ interaction among various on/off switches to perform different logical functions. These gates have inputs that embody two or more simple on/off switches and internal "circuitry" that generates a certain output based on the state of the input switches.

An excellent example of such a molecule is **14** (Fig. 10), which consists of three covalently-linked photochromes.[54,55] Molecule **14** bears two fulgimides and a dithienylethene (DTE). Dithienylethenes are photochromes that, like the fulgimides, are thermally metastable in either isomeric form (DTEo or DTEc), but can be interconverted with light of the appropriate wavelengths. Each of the photochromes of **14** may exist in two photoisomeric forms, as shown in Fig. 10. The molecule may therefore exist in six constitutionally isomeric forms (there are stereoisomers as well, but these are not relevant for this discussion). For our purposes, only the four isomers in which the two identical fulgimides are in the same form (open or closed) are of importance: FGo-DTEo, FGc-DTEo, FGo-DTEc, and FGc-DTEc. As shown in Fig. 11, each isomer of **14** has a unique spectral signature in absorption and emission. Thus, if **14** is present as a solution in a suitable solvent, such as 2-methyltetrahydrofuran, wavelengths may be chosen which will convert any mixture of isomers to a solution that is very highly enriched in any of the four forms. Such wavelengths and the corresponding interconversions are identified in Fig. 12.

It is important to note that isomer FGc-DTEc does not show FGc emission, whereas FGc-DTEo does. This is because the molecule was designed so that singlet excitation energy is rapidly (τ < 5 ps) transferred from ^{1}FGc to DTEc, thus quenching the fluorescence. This behaviour is achievable only in a covalently linked system, and is vital for several logic functions of **14**.

Triad **14** can function as a photochemical Boolean AND gate. The logical truth table in Table 1 illustrates the requirements for the AND function. The gate has two binary inputs, either of which may be in the OFF (0) or ON (1) state. The gate output is a signal reflecting the result of the AND logic operation: the output turns ON (1) only if both inputs have been switched ON. A solution of **14** can operate as a supramolecular photochemical AND gate, as shown in Fig. 13. The initial state is FGo-DTEo, the inputs are light pulses at 397 nm and 302 nm, and the output is absorbance at 535 nm above a threshold value (dashed line in Fig. 13). An ON output above the threshold is observed only after both inputs have been applied. Chemically, this occurs because only the two inputs together, applied at the same time or in any sequence, generate isomer FGc-DTEc (Fig. 12). This is the only isomer having the necessary absorbance at 535 nm (Fig. 11). Other combinations of inputs give outputs at levels below the threshold, corresponding to subthreshold leakage currents in a transistor.

Molecule **14**, is unique among molecular logic machines in that it can be reconfigured to carry out a total of 13 different logic operations. All of these operations have the same initial state, FGo-DTEo. Reconfiguring simply requires changing the input and output wavelengths as required. In fact, the compound can even perform several operations simultaneously by monitoring several outputs at once.

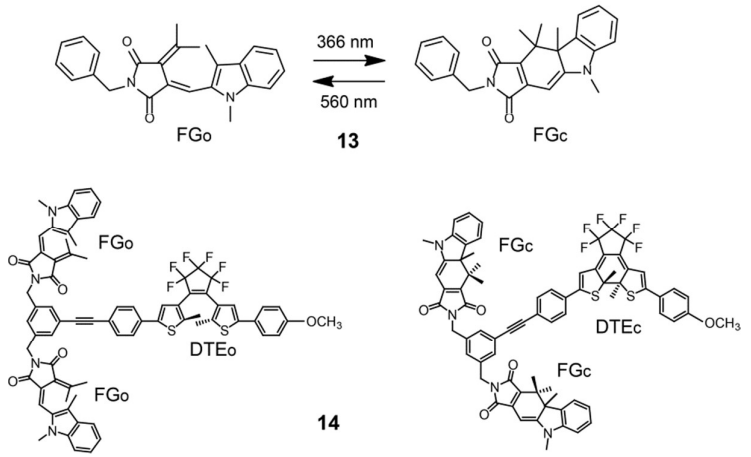

Fig. 10. Molecules for molecular logic include fulgimide (FG) photochemical switch **13** and multifunctional logic gate **14**.

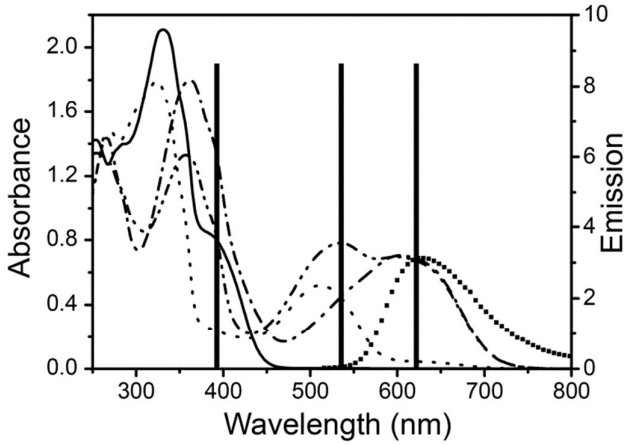

Fig. 11. Absorption and emission spectra of different forms of FG-DTE triad **14**. Solid line: thermally stable FGo-DTEo. Dotted line: FGc-DTEo. Dash-dot: FGo-DTEc. Dash-dot-dot: FGc-DTEc. Also shown is the emission from FGc in the FGc-DTEo form of the molecule (squares). The solid vertical lines indicate wavelengths that are used as outputs for the Boolean logic functions of the supramolecular photochemical logic gate.

Four of the operations of **14** are simple Boolean logic gates: AND, XOR (exclusive OR), and two INH (inhibit) gates. The AND and XOR gate functions share the same inputs, and may be concatenated to give a logical half-adder, which adds two binary digits.[55] If the XOR function is combined with either of the INH gates, a binary half-subtractor results.

Table 1 Truth table for binary arithmetic functions. Wavelengths (nm) for the various inputs and outputs (absorption *A* or emission *Em*) are shown on the third line.

Inputs		Outputs			
a	*b*	AND	XOR	INH1	INH2
397	302	*A* 535	$\lvert\Delta A\rvert$ 393	*A* 393	*Em* 624
0	0	0	0	0	0
1	0	0	1	0	1
0	1	0	1	1	0
1	1	1	0	0	0

Triad **14** can also perform non-arithmetic logic operations. These include a digital 2:1 multiplexer. Multiplexers are analogous to mechanical rotary switches that connect any one of several inputs to a single output. If the inputs are reconfigured, the molecule can act as a digital demultiplexer, a single-bit 4-to-2 encoder, a 2-to-4 decoder,[56] and a set of two transfer gates.

Finally, **14** can act as a keypad lock, again with the initial state FGo-DTEo. In a keypad lock, functionally analogous to a keypad lock used on a door, turning the output ON (unlocking the door) depends not only on the state of the inputs, but also on the order in which they are applied. In this case, the inputs are red light at >615 nm and UV light at 366 nm. The output of the lock is fluorescence emission of FGc at 624 nm. Of the 8 possible ordered combinations of the two inputs, only 1 opens the lock.[55]

Although supramolecular digital logic devices are not expected to substitute for their electronic analogues in the foreseeable future, they are quite different from electronic devices in both their structure and their modes of operation. Because they operate at the nanoscale and require no wires or similar connections, they may be applied in an almost unlimited variety of milieus. For example, molecular photonic switches have been used to specifically label micro-objects so that they can be differentiated in solution.[57] Molecular logic systems are in principle compatible with biological systems. Photonic switches could be used to initiate drug delivery only at certain sites (for example a volume element where light beams of two different colours intersect). They could also be used to track the history of nanoparticles (biological or non-biological) circulating in complex flow systems. Because they are non-metallic and are not influenced by low-frequency electromagnetic radiation, they can be applied where conventional electronics are not suitable. Doubtless many more possible applications will arise as the field becomes more mature.

Supramolecular photochemical analog devices. As mentioned above, transistors can act both as digital switches and as analogue amplifiers or signal transducers. In the latter mode, the device again has inputs and outputs, but the output magnitude is a continuously variable function of the magnitude of one of the inputs. The triode amplifier tube or its transistor analogue are examples. Although the properties of a single molecule are quantized by nature, it is possible to employ ensembles of photochemically active supramolecular devices in this analogue fashion.[58,59]

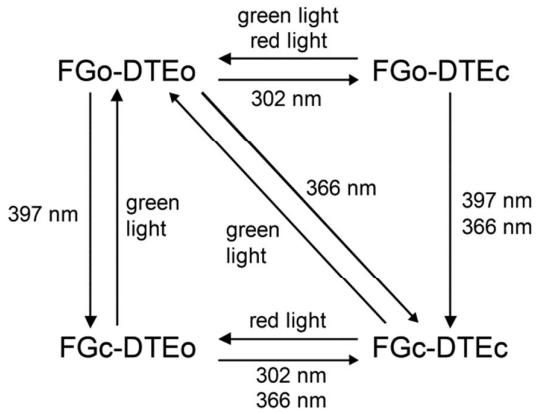

Fig. 12. Photochemical interconversions of the four relevant isomers of **14** and the excitation wavelengths necessary to implement them. Irradiation at a given wavelength yields a photostationary distribution highly enriched in the indicated isomer.

Molecular dyad **15** (Fig. 14) is an example of such a device.[59] It consists of a BDPY moiety, which is a strong fluorophore, covalently linked to a spiro[azahomoadamantane] spirooxazine photochrome. Irradiation of merocyanine form **15o** into its absorption band in the 550 – 610 nm region photoisomerizes the molecule into the spirooxazine form **15c**. When irradiation ceases, **15c** thermally returns to the **15o** form. The time constant for thermal isomerization at 300 K is 4.4 s.

If **15** in acetonitrile is irradiated in the 400 - 500 nm region, where the BDPY moiety absorbs strongly, BDPY fluorescence is observed with maxima at 540 and 577 (sh) nm. In the spirooxazine form **15o**, the fluorescence of the BDPY is not affected by the spirooxazine. However, in the thermally stable merocyanine form of the molecule, **15o**, the merocyanine quenches the BDPY excited singlet state with a rate constant of 1.9×10^8 s^{-1} and a quantum yield of 0.55.

To summarize the photochemistry of **15**, in the thermally stable merocyanine form **15o** the BDPY fluorescence is quenched by the merocyanine. Excitation of the merocyanine photoisomerizes the molecule to the **15c** spirooxazine form, wherein the BDPY fluorescence is not quenched. Thermally, **15c** rapidly reverts to **15o**.

The interchromophore communication between the merocyanine and the BDPY in **15** which results in BDPY fluorescence quenching, coupled with the photoisomerization and rapid thermal reversion of the spirooxazine-merocyanine, makes it possible to modulate the shorter-wavelength fluorescence of the BDPY by secondary excitation with the longer-wavelength light absorbed only by the merocyanine. An example is shown in Fig. 15. In these experiments, fluorescence of the BDPY at 540 nm (shown in the Fig.) was elicited by excitation of BDPY with light of constant intensity at 500 nm in an acetonitrile solution of **15**. At the same time, the sample was excited with square-wave modulated light in the 550-610 nm region, which excites the merocyanaine. With a modulation period of 80 s (Fig. 15a), the fluorescence intensity as a function of time is close to a square wave of the same period. With a modulation frequency of 1.0 s (Fig. 15b), the fluorescence was modulated as a distorted square wave of the same period and reduced modulation depth. Also, there was an induction period after the modulation was turned on during which time the sample reached an average photostationary distribution.

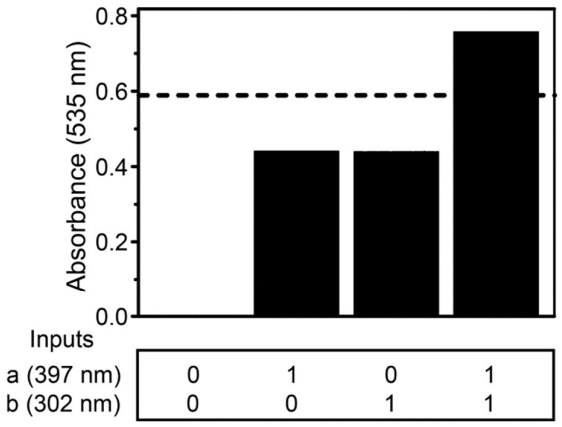

Fig. 13. Performance of triad **14** as a Boolean AND gate. The black bars show the absorbance at 535 nm of a solution of **14** in 2-methyltetrahydrofuran following excitation of the FGo-DTEo form with the combination of input irradiations indicated as *a* and *b* (where 0 means the input is OFF, and 1 means that it is ON). The top of each black bar shows the actual noise level of the measurement. The horizontal dashed line indicated a threshold. The output is ON only if the absorbance is above the threshold value.

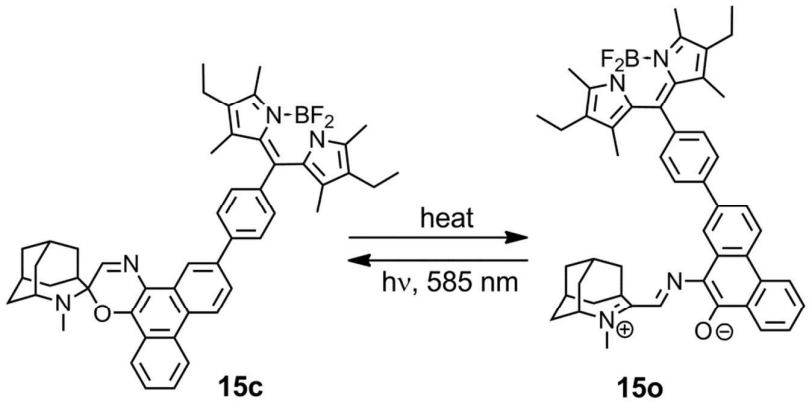

Fig. 14. Closed (**15c)** and open (**15o**) structures of dyad consisting of a BDPY fluorophore covalently linked to a spirooxizine photochrome. Thermally stable merocyanine form **15o** is photochemically isomerized to the spirooxazine form **15c**, which rapidly thermally opens back to the merocyanine.

Modulation with other waveforms is also possible. Fig. 16a shows the results of modulation of the same solution with a sine wave of yellow light (550 – 610 nm, 0-3 mW) having a period of 23 s. The BDPY fluorescence is modulated in a sine wave of the same frequency. Modulation of the yellow light at a frequency of 3.6 s (Fig. 16b) results in BDPY fluorescence with a sine wave of the same period, but lower amplitude and smaller modulation depth.

It should be noted that in **15**, the intensity of shorter-wavelength emission is modulated by longer-wavelength irradiation. This is thermodynamically not possible for a single chromophore with single-photon excitation. It can only happen because of the communication of the BDPY and spirooxazine chromophores and consequent BDPY fluorescence quenching. The supramolecular nature of the system is the key to functionality. Effects of this type may be useful in fluorescence imaging, where phase-sensitive detection could eliminate background noise due to absorption of the light exciting fluorescence by other components followed by emission by these components. An example of such interference is "autofluorescence" of biological samples.

Applying photochemical molecular logic to artificial photosyinthesis.

Thus far, we have illustrated supramolecular photochemistry with examples from artificial photosynthesis and molecular logic. In conclusion, we will discuss an example of the confluence of these two disciplines, in the mimicry of photosynthetic photoregulation.

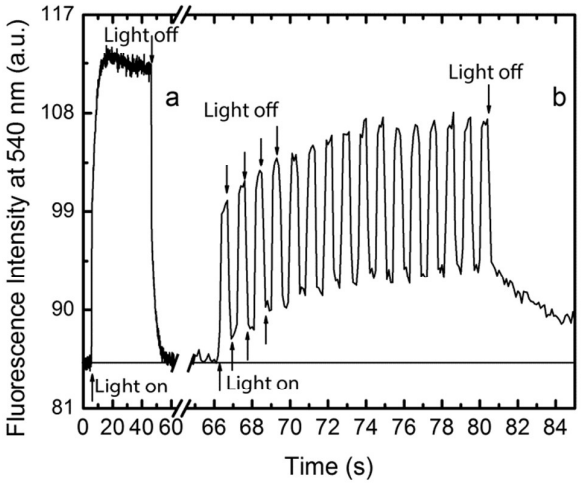

Fig. 15. Square wave modulation experiments with **15** in acetonitrile at 300 K. Fluorescence of the BDPY moiety at 540 nm (shown here) was elicited by excitation with steady intensity light at 500 nm, and the sample was also excited with longer-wavelength square-wave modulated light (550-610 nm) with periods of (a) 80 s and (b) 1 s.

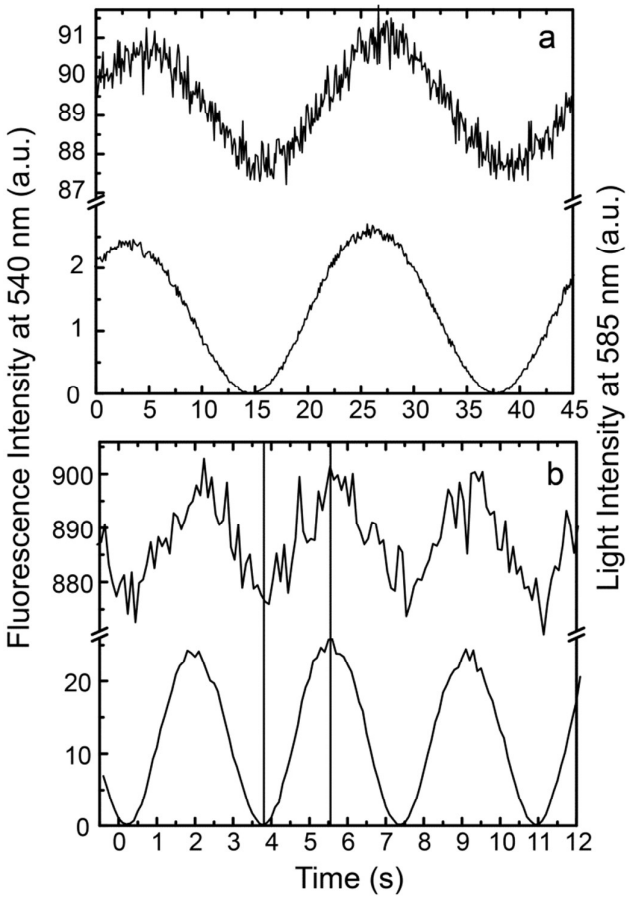

Fig. 16. Sine wave modulation experiments with **15** in acetonitrile at 300 K. Fluorescence of the BDPY moiety at 540 nm (upper curves, left axis) was elicited by excitation with steady intensity light at 500 nm, and the sample was also excited with sine wave modulated light (550-610 nm, lower curves, right axis) (a) Modulation period of 23 s (b) Modulation period of 3.6 s. The vertical lines in (b) illustrate the lack of a significant phase shift in these experiments.

Under conditions of bright sunlight the antenna systems of photosynthetic organisms collect far more light than can be used by the reaction centres. Although this function is useful at low light intensities, at high light it results in the photogeneration of oxidation and reduction equivalents by the reaction centres more rapidly than the dark, catalytic reactions can use the resulting stored energy to make fuels. The result is photodamage due to these high energy intermediates and their reaction products. Photosynthetic organisms have developed various mechanisms for regulating photosynthesis as a function of light intensity. One of these mechanisms is called non-photochemical quenching (NPQ). The process takes different forms in different organisms. The phycobilisome antenna system of cyanobacteria contains a soluble carotenoid protein called orange carotenoid protein that is involved in the NPQ process.[60,61] Under low light conditions, this protein is orange in color and has no effect on the photosynthetic process. Under high light, the protein converts to a red form, which quenches the excitation collected by the antenna chromophores before it reaches the reaction centre. Thus, the red form down regulates photosynthesis. The red form thermally reverts to the inactive orange form. The amount of protein in the red form increases as the light intensity increases, and decreases as the light intensity decreases. The result is that the quantum yield of the photosynthetic process is reduced as the light intensity increases, and vice-versa.

This general photosynthetic regulatory process has been functionally mimicked using molecular pentad **16** (Fig. 17).[62] Molecule **16** features a porphyrin-fullerene artificial reaction centre much like those discussed earlier. Linked to the porphyrin moiety are two BPEA antennas and a photochromic dye. Under low light conditions, the dye exists in the dihydroindolazine (DHI, **16c**) form, which only absorbs in the blue spectral region and has no effect on the photochemistry of the rest of the molecule. When the DHI absorbs light, it photoisomerizes into a colored betaine (BT), as in **16o**. Molecule **16o** thermally converts back to **16c** with a time constant of 37 s at 25 °C.

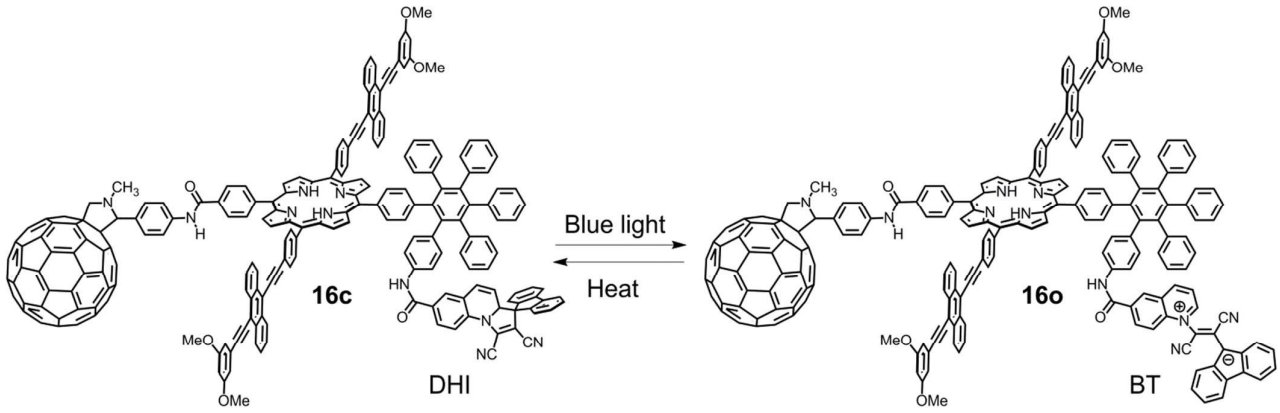

Fig. 17. Pentad **16** features a porphyrin-fullerene artificial reaction centre, two BPEA antennas and a dihydroindolizine photochromic control unit.

Spectroscopic studies of **16** demonstrate that when the porphyrin moiety of **16c** is excited, it donates an electron to the fullerene with a time constant of 2.4 ns to form a charge-separated state with a quantum yield of 0.82. Light absorbed by the BPEA moieties is transferred to the porphyrin with a quantum yield of unity, and also leads to photoinduced electron transfer. Thus, **16c** acts as an efficient artificial photosynthetic antenna-reaction centre combination. When **16c** is isomerized to **16o**, the resulting betaine efficiently quenches the porphyrin first excited singlet state by energy transfer with a time constant of only 33 ps, thus essentially precluding photoinduced electron transfer (Φ = 0.01). The resulting BT excited state decays to the ground state with the liberation of heat.

This behavior allows **16** to mimic NPQ in cyanobacteria. At low light levels, a sample of the compound in solution exists mainly as **16c** and undergoes photoinduced electron transfer with a quantum yield of 0.82. As the light intensity is raised, increasing amounts of the **16c** are converted to **16o**, which has a quantum yield of charge separation of only 1%, and the overall yield of charge separation for the solution decreases. When the light intensity is lowered again, the overall yield increases. This behavior is shown in Fig. 18, which shows the results of 13 experiments in which a sample of **16** dissolved in 2-methyltetrahydrofuran was illuminated with white light of various intensities. At low light, the quantum yield of photoinduced electron transfer was 0.82, but at the highest intensities investigated, it was reduced to 0.37. Lowering the light level returned the quantum yield to its initial value. Thus, **16** reversibly decreases the quantum yield of charge separation in the solution as the light intensity increases. This behavior is functionally analogous to the way that orange carotenoid protein controls the yield of photosynthesis in cyanobacteria.

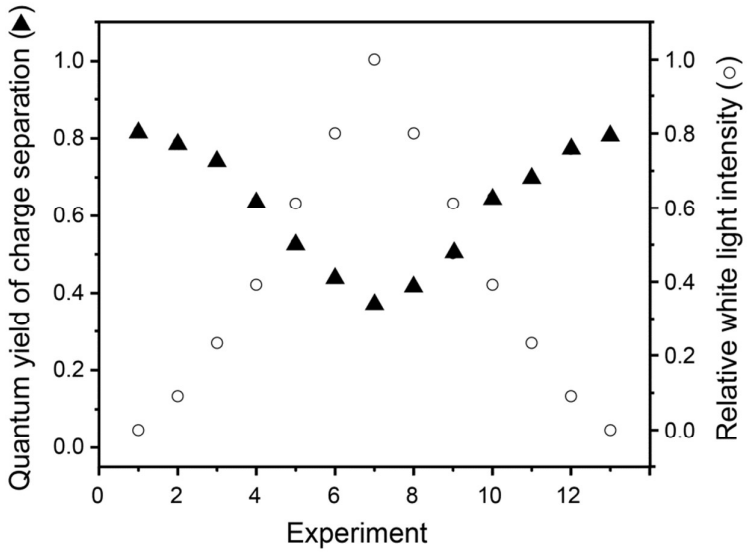

Fig. 18. Results from a sample of pentad **16** in 2-methyltetrahydrofuran following irradiation with different white light fluxes (○, right axis). The quantum yield of photoinduced electron transfer for the solution (●, left axis) decreases as the white light intensity increases because white light converts increasing amounts of pentad **16c** to **16o**, in which the porphyrin excited singlet state lifetime is quenched and the yield of photoinduced electron transfer reduced.

Conclusions

We have seen that supramolecular photochemical devices consist of chromophores, donors and acceptors that are associated in such a way that the component moieties interact by mechanisms such as, but not limited to, singlet or triplet energy transfer, photoinduced electron transfer and exchange of spin information. By choosing the moieties and controlling their modes of interaction, the supramolecular photochemist can demonstrate scientifically interesting and potentially useful phenomena that are not possible in simpler systems. The association mechanism(s) include not only a variety of non-bonded interactions but also linkages through chemical bonds that are not part of the active components. The examples given here are limited in that they deal only with artificial photosynthesis, molecular logic, and spin-spin interactions and most of them come from the same laboratory. The field as a whole is amazingly rich, involving a wide variety of component types, association mechanisms, interactions among components, and potential applications.

Acknowledgements

This work was supported by the Office of Basic Energy Sciences, Division of Chemical Sciences, Geosciences, and Energy Biosciences, Department of Energy under contract DE-FG02-03ER15393.

Notes and references

1 J.-M. Lehn, *Angew. Chem. ,Int. Ed.*, 1988**, 27**, 89-112.
2 V. Balzani, L. Moggi, and F. Scandola, in *Supramolecular Photochemistry*, ed.V. Balzani, D. Reidel, Dordrecht, 1987, pp. 1-28.
3 *Supramolecular Photochemistry,* ed. V. Balzani, D. Reidel, Dordrecht, 1987.
4 T. Förster, *Ann. Physik*, 1948**, 2**, 55-75.
5 T. Förster, *Disc. Faraday Soc.*, 1959**, 27**, 7-17.
6 R. A. Marcus, *J. Chem. Phys.*, 1956**, 24**, 966-978.
7 R. A. Marcus and N. Sutin, *Biochim. Biophys. Acta*, 1985**, 811**, 265-322.
8 V. Levich, *Adv. Electrochem. Electrochem. Eng.*, 1966**, 4**, 249-371.
9 N. S. Hush and J. Ulstrup, *Some historical notes on chemical charge transfer*, School of Chemistry,The University of Sydney,Australia, 1997.
10 N. S. Hush, *Trans. Faraday Soc.*, 1961**, 57**, 557-580.
11 N. S. Hush, *J. Chem. Phys.*, 1958**, 28**, 962-972.
12 H. Mcconnell, *J. Chem. Phys.*, 1961**, 35**, 508-515.
13 D. L. Dexter, *J. Chem. Phys.*, 1953**, 21**, 836-850.
14 G. S. Engel, T. R. Calhoun, E. L. Read, T. K. Ahn, T. Mancal, Y. C. Cheng, R. E. Blankenship, and G. R. Fleming, *Nature*, 2007**, 446**, 782-786.
15 A. Ishizaki and G. R. Fleming, *Proc. Natl. Acad. Sci. U. S. A.*, 2009**, 106**, 17255-17260.
16 Y. Fujihashi, G. R. Fleming, and A. Ishizaki, *J. Chem. Phys.*, 2015**, 142**, 212403-1-212403-11.
17 G. S. Schlau-Cohen, A. Ishizaki, T. R. Calhoun, N. S. Ginsberg, M. Ballottari, R. Bassi, and G. R. Fleming, *Nat. Chem.*, 2012**, 4**, 389-395.
18 U. E. Steiner and T. Ulrich, *Chem. Rev.*, 1989**, 89**, 51-147.
19 C. B. Grissom, *Chem. Rev.*, 1995**, 95**, 3-24.
20 R. E. Blankenship, T. J. Schaafsma, and W. W. Parson, *Biochim. Biophys. Acta*, 1977**, 461**, 297-305.
21 A. J. Hoff, *Photochem. Photobiol.*, 1986**, 43**, 727-745.
22 S. G. Boxer, C. E. D. Chidsey, and M. G. Roelofs, *J. Am. Chem. Soc.*, 1982**, 104**, 1452-1454.
23 B. van Dijk, J. K. H. Carpenter, A. J. Hoff, and P. J. Hore, *J. Phys. Chem. B*, 1998**, 102**, 464-472.
24 D. Kuciauskas, P. A. Liddell, A. L. Moore, T. A. Moore, and D. Gust, *J. Am. Chem. Soc.*, 1998**, 120**, 10880-10886.
25 K. Maeda, K. B. Henbest, F. Cintolelsi, I. Kuprov, C. T. Rodgers, P. A. Liddell, D. Gust, C. R. Timmel, and P. J. Hore, *Nature*, 2008**, 453**, 387-390.
26 K. Maeda, C. J. Wedge, J. G. Storey, K. B. Henbest, P. A. Liddell, G. Kodis, D. Gust, P. J. Hore, and C. R. Timmel, *Chem. Commun.*, 2011**, 47**, 6563-6565.
27 G. Ciamician, *Science*, 1912**, 36**, 385-394.
28 Y. Terazono, G. Kodis, P. A. Liddell, V. Garg, T. A. Moore, A. L. Moore, and D. Gust, *J. Phys. Chem. B*, 2009**, 113**, 7147-7155.
29 J. L. Kong and P. A. Loach, *J. Heterocyclic Chem.*, 1980**, 17**, 737-744.
30 J. L. Kong, K. G. Spears, and P. A. Loach, *Photochem. Photobiol.*, 1982**, 35**, 545-553.
31 J. L. Kong and P. A. Loach, in *Frontiers of Biological Energetics: From Electrons to Tissues*, ed.P. L. Dutton, Scarpa H., Academic Press, New York, 1978, pp. 73-82.

32 I. Tabushi, N. Koga, and M. Yanagita, *Tetrahedron Lett.*, 1979257-257.
33 V. Garg, G. Kodis, M. Chachisvilis, M. Hambourger, A. L. Moore, T. A. Moore, and D. Gust, *J. Am. Chem. Soc.*, 2011**, 133**, 2944-2954.
34 D. Kuciauskas, P. A. Liddell, S. Lin, S. Stone, A. L. Moore, T. A. Moore, and D. Gust, *J. Phys. Chem. B*, 2000**, 104**, 4307-4321.
35 H. Imahori, *Org. Biomol. Chem.*, 2004**, 2**, 1425-1433.
36 D. M. Guldi, *Chem. Soc. Rev.*, 2002**, 31**, 22-36.
37 E. Maligaspe, T. Kumpulainen, N. K. Subbaiyan, M. E. Zandler, H. Lemmetyinen, N. V. Tkachenko, and F. D'Souza, *Phys. Chem. Chem. Phys.*, 2010**, 12**, 7434-7444.
38 D. Gust, P. Mathis, A. L. Moore, P. A. Liddell, G. A. Nemeth, W. R. Lehman, T. A. Moore, R. V. Bensasson, E. J. Land, and C. Chachaty, *Photochem. Photobiol.*, 1983**, 37S**, S46-S46.
39 T. A. Moore, D. Gust, P. Mathis, J. C. Mialocq, C. Chachaty, R. V. Bensasson, E. J. Land, D. Doizi, P. A. Liddell, W. R. Lehman, G. A. Nemeth, and A. L. Moore, *Nature*, 1984**, 307**, 630-632.
40 S. Nishitani, N. Kurata, Y. Sakata, S. Misumi, A. Karen, T. Okada, and N. Mataga, *J. Am. Chem. Soc.*, 1983**, 105**, 7771-7772.
41 D. Gust, T. A. Moore, A. L. Moore, P. A. Liddell, D. Kuciauskas, J. P. Sumida, B. Nash, and D. Nguyen, in *Recent Advances in the Chemistry and Physics of Fullerenes and Related Materials*, ed.K. M. Kadish, A. W. Rutherford, The Electrochemical Society, Pennington, NJ, 1997, vol. 4, pp. 9-24.
42 G. Kodis, P. A. Liddell, A. L. Moore, T. A. Moore, and D. Gust, *J. Phys. Org. Chem.*, 2004**, 17**, 724-734.
43 H. Imahori, Y. Sekiguchi, Y. Kashiwagi, T. Sato, Y. Araki, O. Ito, H. Yamada, and S. Fukuzumi, *Chem. Eur. J.*, 2004**, 10**, 3184-3196.
44 S. M. Molnar, G. Nallas, J. S. Bridgewater, and K. J. Brewer, *J. Am. Chem. Soc.*, 1994**, 116**, 5206-5210.
45 C. Chiorboli, S. Fracasso, F. Scandola, S. Campagna, S. Serroni, R. Konduri, and F. M. MacDonnell, *Chem. Commun.*, 20031658-1659.
46 R. Konduri, H. W. Ye, F. M. MacDonnell, S. Serroni, S. Campagna, and K. Rajeshwar, *Angew. Chem. ,Int. Ed.*, 2002**, 41**, 3185-3187.
47 H. A. Frank, J. Machnicki, and R. A. Friesner, *Photochem. Photobiol.*, 1983**, 38**, 451-455.
48 C. C. Schenck, P. Mathis, and M. Lutz, *Photochem. Photobiol.*, 1984**, 39**, 407-417.
49 L. Takiff and S. G. Boxer, *J. Am. Chem. Soc.*, 1988**, 110**, 4425-4426.
50 R. V. Bensasson, E. J. Land, A. L. Moore, R. L. Crouch, G. Dirks, T. A. Moore, and D. Gust, *Nature*, 1981**, 290**, 329-332.
51 S. Johnsen and K. J. Lohmann, *Nat. Rev. Neurosci.*, 2005**, 6**, 703-712.
52 K. Schulten and A. Weller, *Biophys. J.*, 1978295-305.
53 S. D. Straight, Y. Terazono, G. Kodis, T. A. Moore, A. L. Moore, and D. Gust, *Aust. J. Chem.*, 2006**, 59**, 170-174.
54 S. D. Straight, P. A. Liddell, Y. Terazono, T. A. Moore, A. L. Moore, and D. Gust, *Adv. Funct. Mater.*, 2007**, 17**, 777-785.
55 J. Andréasson, U. Pischel, S. D. Straight, T. A. Moore, A. L. Moore, and D. Gust, *J. Am. Chem. Soc.*, 2011**, 133**, 11641-11648.
56 J. Andréasson, S. D. Straight, T. A. Moore, A. L. Moore, and D. Gust, *J. Am. Chem. Soc.*, 2008**, 130**, 11122-11128.
57 A. P. de Silva, M. R. James, B. O. F. McKinney, D. A. Pears, and S. M. Weir, *Nat. Mater.*, 2006**, 5**, 787-790.
58 A. E. Keirstead, J. W. Bridgewater, Y. Terazono, G. Kodis, S. Straight, P. A. Liddell, A. L. Moore, T. A. Moore, and D. Gust, *J. Am. Chem. Soc.*, 2010**, 132**, 6588-6595.
59 G. Copley, J. G. Gillmore, J. Crisman, G. Kodis, C. L. Gray, B. R. Cherry, B. D. Sherman, P. A. Liddell, M. M. Paquette, L. Kelbauskas, N. L. Frank, A. L. Moore, T. A. Moore, and D. Gust, *J. Am. Chem. Soc.*, 2014**, 136**, 11994-12003.
60 A. Wilson, G. Ajlani, J. M. Verbavatz, I. Vass, C. A. Kerfeld, and D. Kirilovsky, *Plant Cell*, 2006**, 18**, 992-1007.
61 A. Wilson, C. Punginelli, A. Gall, C. Bonetti, M. Alexandre, J. M. Routaboul, C. A. Kerfeld, R. van Grondelle, B. Robert, J. T. Kennis, and D. Kirilovsky, *Proc. Natl. Acad. Sci. U. S. A.*, 2008**, 105**, 12075-12080.
62 S. D. Straight, G. Kodis, Y. Terazono, M. Hambourger, T. A. Moore, A. L. Moore, and D. Gust, *Nat. Nanotechnol.*, 2008**, 3**, 280-283.